

Spatial model for forecast of vehicular emission distribution in urban built-up areas

R.B. Nuterman and A.V. Starchenko

Tomsk State University

Received February 1, 2007

The results of numerical modeling of aerodynamics and pollution transfer in urban built-up areas are presented. The spatial microscale model includes Reynolds equations for aerodynamics prediction and “ k – ε ” two-parametric turbulence model. The numerical solution of the equations is based on the finite volume method. The mathematical model was verified by a set of experiments. Besides, the microscale model was compared with the field data, obtained within the TRAPOS (Optimization of Modeling Methods for Traffic Pollution in Streets) project.

The aim of the work and mathematical statement of the problem

The vehicular emission becomes the main source of the urban air pollution. Street canyons are among key urban elements, where the traffic is relatively heavy and the pollution effect on a human organism increases significantly. The scenario analysis and forecast of air pollution in street canyons allow us to determine adverse conditions with formation of locally high exhaust concentrations, as well as to take into account natural ventilation of urban quarters when planning urban relief.

To investigate the propagation character of gaseous traffic-induced air pollutants in built-up areas, mathematical modeling methods^{1–3} are widely used along with experimental ones; they include hydrodynamic equations, turbulence models, and turbulence diffusion equations. At present, microscale meteorological models are of significantly growing interest owing to prospects of their use to develop reliable schemes of urban boundary layer parameterization for mesoscale atmospheric models.⁴

A spatial microscale model and calculation technique for flows around obstacles and in street canyons are described in this work, as well as their experimental validation.

The microscale aerodynamics and pollutant transfer model is based on stationary three-dimensional Reynolds equations, two-parameter “ k – ε ” turbulence model,⁵ and advection-diffusion equation; principal thermophysical properties are considered here as constant. Mass, momentum, and pollutant concentration conservation equations have the following form:

$$\frac{\partial U_j}{\partial x_j} = 0, \quad (1)$$

$$\frac{\partial(U_i U_j)}{\partial x_j} = -\frac{1}{\rho} \frac{\partial P}{\partial x_i} + \frac{\partial}{\partial x_j} \left[\nu \left(\frac{\partial U_i}{\partial x_j} + \frac{\partial U_j}{\partial x_i} \right) \right] + \frac{\partial(-\overline{u'_i u'_j})}{\partial x_j}, \quad (2)$$

$i = 1, 2, 3,$

$$\frac{\partial(U_j C)}{\partial x_j} = \frac{\partial}{\partial x_j} \left[D \left(\frac{\partial C}{\partial x_j} \right) \right] + \frac{\partial(-\overline{u'_j c'})}{\partial x_j} + S. \quad (3)$$

Here U_i and C are the average components of velocity and pollutant concentration, respectively; u'_i and c' are the fluctuations of components of velocity and concentration; ρ is the liquid density; P is the pressure; ν and D are the molecular kinematic viscosity and molecular diffusion, respectively; x_i are the Cartesian coordinates; S is the constant intensity source. The summation from 1 to 3 in Eqs. (1)–(3) is carried out over the repetitive index j .

Reynolds stress $\overline{u'_i u'_j}$ and turbulent diffusion flows $\overline{u'_j c'}$ are modeled using the Boussinesq closure relations:

$$\overline{u'_i u'_j} = -\nu_t \left(\frac{\partial U_i}{\partial x_j} + \frac{\partial U_j}{\partial x_i} \right) + \frac{2}{3} k \delta_{ij},$$

$$\overline{u'_j c'} = -\Gamma_t \frac{\partial C}{\partial x_j}, \quad \delta_{ij} = \begin{cases} 1, & i = j, \\ 0, & i \neq j. \end{cases}$$

The two-parametric turbulence model has the following form⁵:

$$U_j \frac{\partial k}{\partial x_j} = \nu_t \left(\frac{\partial U_i}{\partial x_j} + \frac{\partial U_j}{\partial x_i} \right) \frac{\partial U_i}{\partial x_j} + \frac{\partial}{\partial x_j} \left(\frac{\nu_t}{\sigma_k} \frac{\partial k}{\partial x_j} \right) - \varepsilon, \quad (4)$$

$$U_j \frac{\partial \varepsilon}{\partial x_j} = C_1 \nu_t \frac{\varepsilon}{k} \left(\frac{\partial U_i}{\partial x_j} + \frac{\partial U_j}{\partial x_i} \right) \frac{\partial U_i}{\partial x_j} + \frac{\partial}{\partial x_j} \left(\frac{\nu_t}{\sigma_\varepsilon} \frac{\partial \varepsilon}{\partial x_j} \right) - C_2 \frac{\varepsilon^2}{k}, \quad (5)$$

$$\nu_t = C_\mu \frac{k^2}{\varepsilon}, \quad \Gamma_t = \frac{\nu_t}{Sc_t},$$

where k and ε are the turbulent kinetic energy and turbulent dissipation, respectively; constants $C_\mu = 0.09$, $C_1 = 1.44$, $C_2 = 1.92$, $\sigma_k = 1.0$, $\sigma_\varepsilon = 1.3$, and $Sc_t = 0.7$.

Moving vehicles are not only sources of pollutant emissions into the atmosphere, but also generators of the so-called mechanical turbulence, caused by the air disturbance as a result of motion of a finite-length objects having a significant resistance. In this work, this factor is taking into account (like in Ref. 3) by adding the corresponding terms into the “ $k-\varepsilon$ ” turbulence model. To take into account the traffic-induced turbulence kinetic energy, the term $C_{\text{car}}V_{\text{car}}^2Q_{\text{car}}$ is added to the right part of Eq. (4) and the term, responsible for dissipation of turbulence mechanical energy, – to Eq. (5) in the form $C_{\text{car}}V_{\text{car}}^2Q_{\text{car}}(\varepsilon/k)$, where $C_{\text{car}} = 0.0015$ is the empirical coefficient,³ V_{car} is the vehicle speed, Q_{car} is the number of vehicles per second (in calculations $V_{\text{car}} = 8.333$ m/s and $Q_{\text{car}} = 0.347$ [Ref. 6]).

Zero normal derivatives are the edge conditions at the outlet from the area under study and at open side boundaries, while at the entrance and on rigid surfaces they have the following form:

– at the entrance at $x = x_1$:

$$U_1 = U_{in}(x_3), \quad U_2 = U_3 = 0, \quad C = 0, \\ k = k_{in}(x_3), \quad \varepsilon = \varepsilon_{in}(x_3);$$

– on a rigid surface:

$$U_1 = U_2 = U_3 = 0, \quad \frac{\partial C}{\partial n} = 0,$$

where U_{in} , k_{in} , ε_{in} are the known functions of the vertical coordinate x_3 ; n is the vector normal to the boundary; x_3 is the vertical coordinate.

The method of Launder–Spalding wall functions⁵ is used to calculate turbulent parameters of a flow near a wall.

Calculation technique and results

Differential equations are discretized by the finite volume method,⁷ and the convective terms of transfer equations are approximated by the Van Leer MLU scheme.⁸ Integrals are calculated using piecewise-linear profiles, describing variations of a dependent variable between nodes. Such integration results in a discrete analog of differential equations, which contains variable values at several neighboring nodes. To solve it, the fictitious domain method was used, the idea of which is in the fact that vector and scalar quantities in the obstacle area are equal to zero; and the diffusion is lacking in fictitious finite volumes. The system of finite-difference equation is solved by the Buleev explicit method.¹⁰

Flows around bluff bodies include complex phenomena, for example, separation and joining of flows, formation of transient eddy, increased turbulence level. It is natural that there is a practical need in forecasting such flows, though this problem is complicated even for relatively simple geometries.

To test the microscale model of atmospheric boundary layer, a flow around a cube (of the height h , located in a channel of $2h$ in height and $4h$ in

width, a distance between the cube front face and input boundary of $60h$) is considered in this work (Fig. 1). For this geometry, the Reynolds number $Re = U_b h / \nu = 40000$, $U_b = 28.8$ m/s is the average flow speed at the channel entrance. The results of experimental study of this flow are given in Ref. 11. A grid of $97 \times 82 \times 42$ in size was used for calculations, which, along with measurements, have shown that a quite complex flow is observed even for a simple geometry (see Fig. 1).

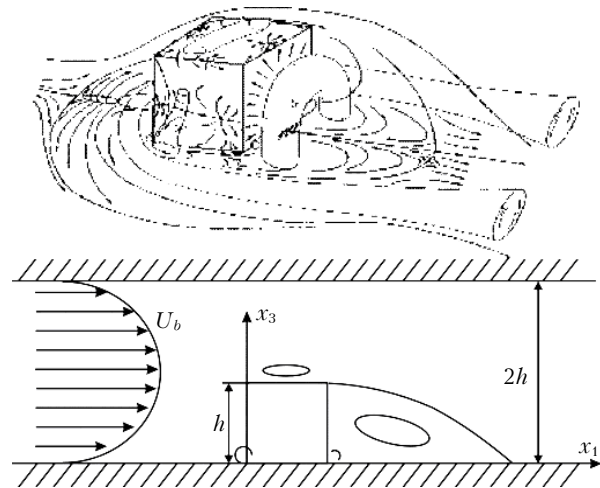


Fig. 1. Schematic view of the flow around the cube.¹¹

While moving, the flow is separated at the cube front face with formation of the secondary recirculations at the upper cube face, near its side faces, and at the lower part of its front face (Fig. 2).

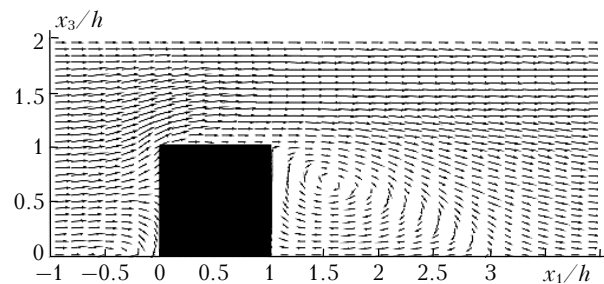


Fig. 2. Vector velocity field at the plane $x_2 = 0$ for the flow around the cube.

The main vortex in the trail behind the cube has a horseshoe shape. A large isolated zone is developed there, interacting with the horseshoe-shaped vortex. In addition, an arc-shaped vortex is formed in the recirculation zone (Figs. 1–3).

Calculations show that the commonly used “ $k-\varepsilon$ ” model inadequately simulates a flow and turbulent structure in the area with recirculation liquid movements (Fig. 4).

This is well seen when considering the kinetic energy level behind the cube (Fig. 5).

Such behavior is explained by the fact that the two-parametric model forecasts significantly less level

of kinetic energy generation behind the obstacle than its real value. As a result, the turbulence viscosity decreases and a vortex trail behind the cube increases. Nevertheless, it can be expected that some modifications of “ $k-\epsilon$ ” model, convenient in calculations, can result in more plausible model data.¹²

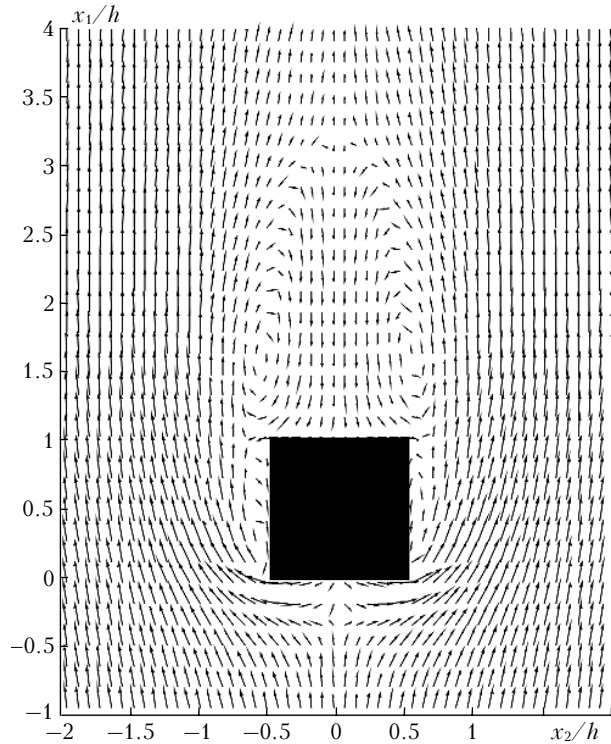


Fig. 3. Vector velocity field for the flow around the cube at $x_3/h = 0.075$.

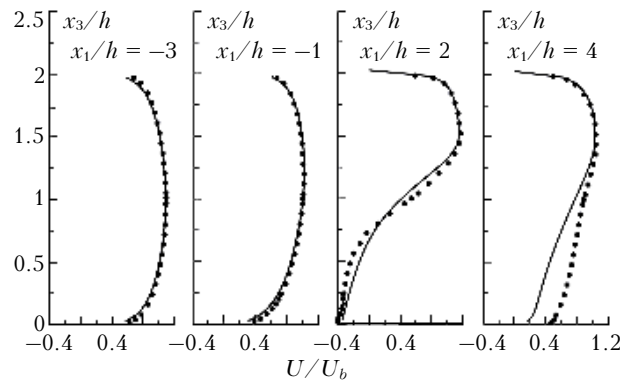


Fig. 4. Longitudinal velocity component U_1 for the flow around the cube: model calculations (—) and experimental data¹¹ (•).

Realizing the importance of testing the mathematical models for solving the problem of pollutant propagation in urban areas, a team of scientists, working within the TRAPOS Project (Optimization of Modeling Methods for Traffic Pollution in Streets),¹³ has prepared a number of tests, including comparison between experimental and calculation results. The most complicated case is the study of pollutant aerodynamics and transfer in the

built-up area around the Gettinger street in Hannover city. The field¹⁴ and laboratory data¹⁵ on the pollutant concentration in a point near some pollutant source, as well as meteorological data recorded over the highest building’s roof are available for solving this problem.

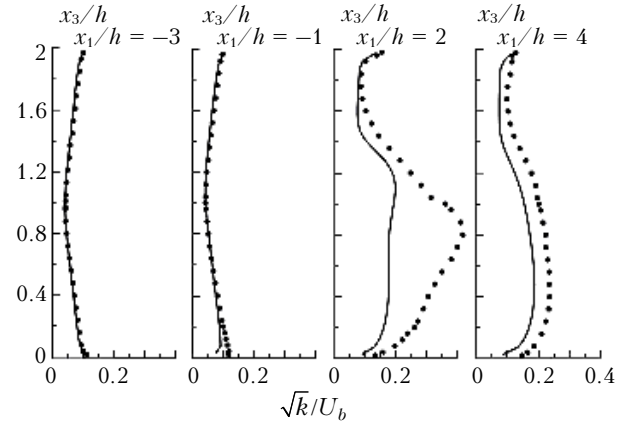


Fig. 5. Turbulent kinetic energy for the flow around the cube: model calculations (—) and experimental data¹¹ (•).

Figure 6 presents the vector field of horizontal velocity component and dimensionless pollutant concentration $c^* = CV_{ref}H/(Q/L)$ ($V_{ref} = 10$ m/s is the characteristic velocity at a height of 100 m; $H = 20$ m is the average building height; Q is the intensity of vehicular emission; $L = 180$ m is the linear source length).

The incoming flow is directed from the south to north. A geometrical model, used for calculations, is a precise replica of the Gettinger street (see Fig. 6). The detailed description of this case, including edge conditions and parameters of the surface roughness have been obtained from Internet (TRAPOS database).¹³ The calculations show a complex turbulent motion of air masses (see Fig. 6). Formation of vortex structures near quoin is seen, as well as air mass involvement in recirculation motion at the opposite side of the street, which results in vehicular pollution accumulation. At such direction of main airflow motion, traffic-induced pollutants do not get to courtyards, but are drifted along the street, increasing the concentration near the left side of the street.

Figure 7 presents the results of comparison of calculated and measured values of wind velocity and turbulent kinetic energy over the meteorological mast (see Fig. 6).

As is evident from Fig. 7, the wind velocity component U_3 is slightly overestimated, while other components virtually perfectly coincide with the measured values. However, the calculated turbulence energy (Fig. 7b) is underestimated in the area close to the roof of the highest building, where experimental data show high levels of k . Addition of the source term (Fig. 7c), simulating traffic-induced generation of turbulence energy, results in the increase of total turbulence level, though the underestimation of k remains.

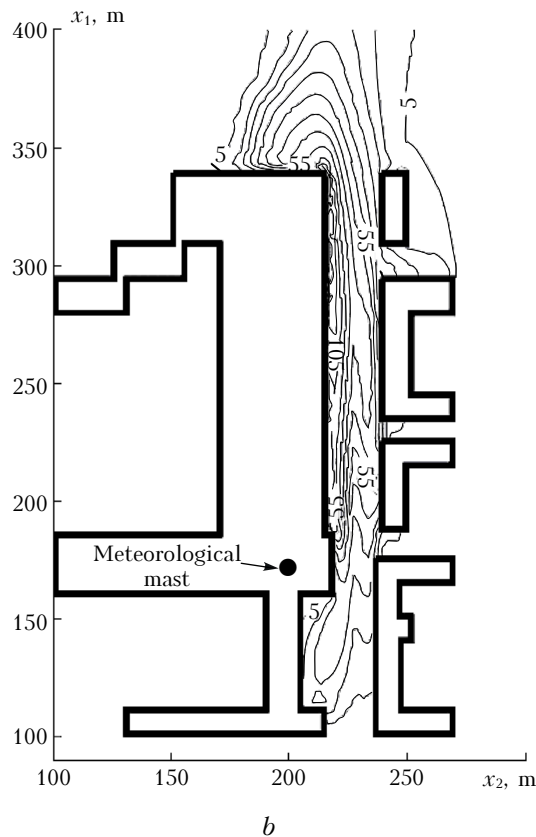
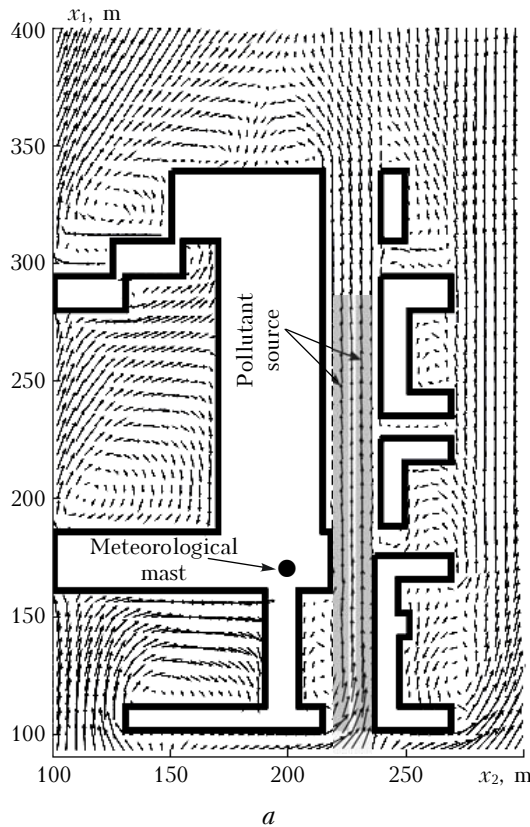


Fig. 6. Surface velocity field (a) and concentration levels (b) in the Gettinger street; ● marks a meteorological mast ($x_3 = 10.5$ m).

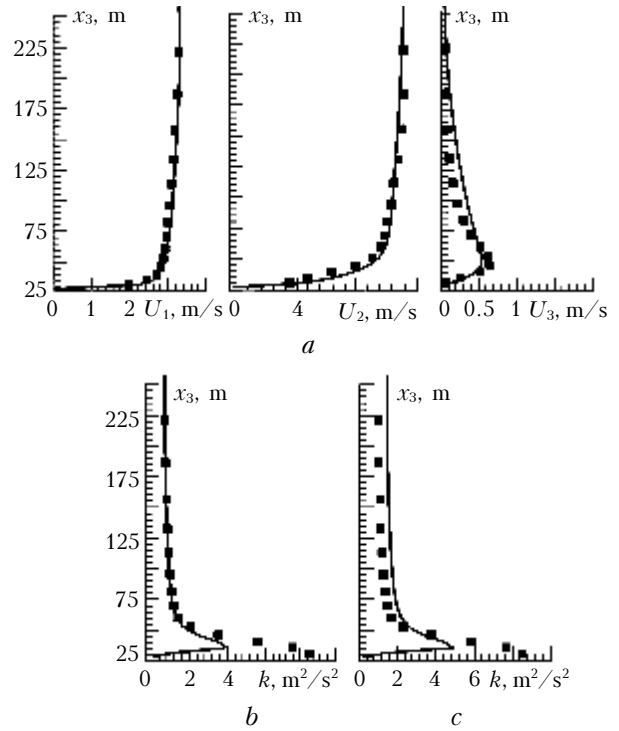


Fig. 7. Wind velocity components (a) and kinetic energy with (c) and without (b) mechanical turbulence: model calculations (—) and experimental data¹⁵ (■).

Conclusion

The results of application of the microscale aerodynamics and pollutant transfer model in built-up areas are presented. The calculations for two complicated geometries were carried out; advantages and disadvantages of the model were revealed. It was shown that the standard “ $k-\epsilon$ ” model reproduced recirculation flows inadequately. In addition, the effect of traffic, generating additional turbulence, on the flow turbulent structure has been studied for the real case. A good agreement with experimental data was obtained. However, the suggested mathematical model for flow turbulent parameters is to be improved, because small differences in flow pattern and velocity direction can result in incorrect forecast of traffic-induced pollutant propagation in urban built-up areas.

Acknowledgements

This work was fulfilled under financial support of INTAS (INTAS Ref. No. 06–100016–5928) and the Russian Foundation for Basic Research (Project No. 07–05–01126).

References

1. T.R. Oke, *Boundary Layer Climates* (Gidrometeoizdat, Leningrad, 1982), 360 pp.
2. R.B. Nuterman and A.V. Starchenko, Proc. SPIE **5396**, 89–98 (2004).

3. R.B. Nuterman and A.V. Starchenko, *Atmos. Oceanic Opt.* **18**, No. 8, 581–588 (2005).
4. A.A. Baklanov and P.G. Mestayer, DMI Scientific Report, Nos. 04–05, 75 (2004).
5. B.E. Launder and D.B. Spalding, *Comput. Methods in Appl. Mechan. and Eng.* **3**, No. 2, 269–289 (1974).
6. P. Louka, “*Contribution of Petrova Louka to the TRAPOS WG-TPT Meeting in Cambridge*,” URL: <http://www2.dmu.dk/atmosphericenvironment/trapos/louka-camb.pdf>
7. S. Patankar, *Computational Methods for Heat Exchange and Flow Dynamics Problems* (Energoatomizdat, Moscow, 1984), 152 pp.
8. B. Noll, *AIAA J.* **30**, No. 1, 64–69 (1992).
9. A.O. Esaulov and A.B. Starchenko, “*Choice of a Scheme for Numerical Solution of Transfer Equations*,” in: *Computational Hydrodynamics* (Publishing House of Tomsk State University, Tomsk, 1999), pp. 27–32.
10. V.P. Il'in, *Methods of Incomplete Factorization for Solution of Algebraic Systems* (Fizmatlit, Moscow, 1995), 288 pp.
11. R. Martinuzzi and C. Tropea, *J. Fluid Eng.* **115**, 85 (1993).
12. W. Rodi, *J. Wind Eng. and Industr. Aerodyn.* **69**, No. 71, 55–75 (1997).
13. URL: <http://www2.dmu.dk/atmosphericenvironment/trapos/>
14. C. Chauvet, B. Leiti, and M. Schatzmann, “*High Resolution Measurements in an Idealised Street Canyon*,” in: *Proc. of the 3rd Int. Conf. on Urban Air Quality*. Loutraki, Greece, March 2001.
15. J. Liedtke, B. Leiti, and M. Schatzmann, “*Dispersion in a Street Canyon: Comparison of Wind Tunnel Experiments With Field Measurements*”, in: *Proc. of Eurotrac Symp.* 98 (WIT Press, 1999), pp. 806–810.